N02

Proceedings of the 5th International Conference on Inverse Problems in Engineering: Theory and Practice, Cambridge, UK, 11-15th July 2005

AN EXPERIMENTAL STUDY ON IDENTIFICATION OF DELAMINATION IN COMPOSITE MATERIAL BY THE PASSIVE ELECTRIC POTENTIAL CT METHOD

K. NAKATANI[1], S. KUBO[1], T. SAKAGAMI[1], D. SHIOZAWA[2] and M. TAKAGI[1]
[1] *Department of Mechanical Engineering and Systems, Graduate School of Engineering, Osaka University, 2-1, Yamadaoka, Suita, Osaka 565-0871 Japan*
[2] *Department of Mechanical Engineering, Kobe University, 1-1, Rokkoudai-cho Nadaku, Kobe, Hyogo 658-8501 Japan*
e-mail: kubo@mech.eng.osaka-u.ac.jp

Abstract - When a piezoelectric film is glued on the surface of a structure member subjected to mechanical load, a distribution of electric potential is induced. In the existence of defects in the member, a characteristic variation of electric potential is observed. Based on this phenomenon, the passive electric potential CT (computed tomography) method is developed for detecting and identifying defects in a structure. In this study, the applicability of the passive electric potential CT method to the identification of a delamination in a CFRP laminate was experimentally examined. CFRP laminate specimens, which have an artificial interlaminar delamination, were prepared. CFRP laminate specimens with a piezoelectric film on their surface were subjected to three-point bending. The electric potential distribution on the piezoelectric film was measured by a non-contact voltmeter. Characteristic variation reflecting the location and the size of the delamination are observed in the measured electric potential distributions on the piezoelectric film. The effect of the depth of the delamination was also observed. These tendencies of variations in measured electric potentials were similar to those found in the potential calculated by the FEM. In order to identify the delamination from the measured electric potential distribution, an inverse method was constructed based on the least squares residual evaluated between the measured and computed electric potential distributions. The location and size of the delamination were estimated accurately. For the estimation of the depth of delamination, the accuracy was deteriorated with increase in the depth. It was shown that the passive electric potential CT method using piezoelectric film is useful for quantitative identification of interlaminar delamination in laminated composite materials.

1. INTRODUCTION

Laminated composites are attractive materials for structural components due to their excellent features, such as high specific strength and stiffness. One of the most common failure modes in laminated composites is delamination, which can result from manufacturing imperfections or can be induced by accidental out-of-plane impact during service. Delamination may considerably degrade properties of composites, especially the compressive strength, resulting in severe decrease in the structural reliability. Delamination detection techniques are therefore necessary to ensure the safety and reliability of the laminated composite structures. Important structures such as aerospace structures require regular inspection process. The inspection process is costly because it requires out-of-service period and skillful operators. Motivated by this, a great deal of research is currently in progress into real-time structural health monitoring (SHM) systems.

In a real-time SHM system, application of a conventional non-destructive evaluation (NDE) technique, such as C-scan or radiographic inspection, is difficult because use of the probes is difficult owing to limitations on space and weight of in-service structures. Therefore, damage evaluation methods proposed for SHM system commonly use sensor elements bonded on structure surfaces or embedded within structure.

In the last decade, many researchers used piezoelectric materials such as lead-zirconate-titanate (PZT) or polyvinylidene fluoride (PVDF) as sensor/actuator device in health monitoring applications. Piezoelectric materials have two characteristics: direct piezoelectric effect to convert mechanical deformation into electric charge and inverse effect to convert voltage into mechanical deformation.

Keilers and Chang [4, 5] proposed a diagnostic method to identify a delamination in a laminated composite beam with piezoceramics attached to it. In their work, some piezoceramics were used as actuators to dynamically excite beams while others were used as sensors to measure the beam responses. Saravanos and Hopkins [8] conducted analytical and experimental work on damped free vibration of delaminated laminate beams. They presented a model based on generalized laminate theory for accurate predictions of delamination effects on the dynamic characteristics. Valdes and Soutis [1] studied the detection of delaminations in composite beams using piezoceramic actuators and piezoelectric film sensors.

Hu *et al.* [2] investigated the influences of delamination on the vibration characteristic of composite laminates using C^0-type FEM model. Lin and Chang [7] fabricated composite structures with a network of distributed piezoceramics actuators/sensors. These studies focused on the effects of delamination on the dynamic characteristics of laminates.

The present authors developed the passive electric potential CT method [10–12] for quantitative crack identification focused on influences of cracks on the strain distribution on the surface of materials. In this method, a PVDF film is used as a sensor element and is directly attached to the surface of materials. When a cracked material is subjected to mechanical load, existence of cracks influences the distribution of mechanical strain on the surface of the material. The strain distribution is directly converted to electric potential distribution on the PVDF film owing to its greater flexibility compared to the structure. Thus electric potential distribution reflecting crack size, location and shape is observed on the surface of PVDF film. Crack identification from electric potential distributions is conducted by the inverse analyses using the FEM. One of the advantages of this method is that electric energy input is not necessary.

In this paper, we investigate the applicability of the passive electric CT method to identification of delamination in composite materials. The effect of the delamination on the electric potential distribution are investigated both analytically and experimentally. Identification of delamination by inverse analyses follows.

2. FEM ANALYSES OF ELECTRIC POTENTIAL DISTRIBUTION

2.1 Formulation of Numerical Analyses

The FEM computer analysis scheme was developed for coupled elastic and electric potential problem to investigate the relationship between delamination parameters and electric potential distribution on PVDF film. The governing equations of elastic and electric response in the piezoelectric material can be written as [3];

$$\{\boldsymbol{\sigma}\} = [\boldsymbol{C}]\{\boldsymbol{\varepsilon}\} - [\boldsymbol{e}]^{\mathrm{T}}\{\boldsymbol{E}\} \tag{1}$$

$$\{\boldsymbol{D}\} = [\boldsymbol{e}]\{\boldsymbol{\varepsilon}\} + [\boldsymbol{g}]\{\boldsymbol{E}\} \tag{2}$$

where $\{\boldsymbol{\sigma}\}$ is stress vector (6×1) and $\{\boldsymbol{\varepsilon}\}$ is strain vector (6×1), $[\boldsymbol{C}]$, $[\boldsymbol{e}]$ and $[\boldsymbol{g}]$ are stiffness matrix (6×6), piezoelectric coefficient matrix (3×6) and dielectric constant matrix (3×3), respectively. $\{\boldsymbol{E}\}$ is electric field vector (3×1). $\{\boldsymbol{D}\}$ is electric displacement vector (3×1). The static FEM equation, based on eqns. (1) and (2), are expressed as;

$$[\boldsymbol{K}_{uu}]\{\boldsymbol{d}\} + [\boldsymbol{K}_{u\phi}]\{\boldsymbol{\phi}\} = \{\boldsymbol{F}\} \tag{3}$$

$$[\boldsymbol{K}_{u\phi}]\{\boldsymbol{d}\} + [\boldsymbol{K}_{\phi\phi}]\{\boldsymbol{\phi}\} = \{\boldsymbol{Q}\} \tag{4}$$

where $[\boldsymbol{K}_{uu}]$, $[\boldsymbol{K}_{u\phi}]$ and $[\boldsymbol{K}_{\phi\phi}]$ are the mass matrix, displacement electric stiffness matrix and electric stiffness matrix, respectively. $\{\boldsymbol{d}\}$, $\{\boldsymbol{\phi}\}$, $\{\boldsymbol{F}\}$ and $\{\boldsymbol{Q}\}$ are the node displacement vector, the node electric potential vector, the mechanical load vector and the electric load vector, respectively [9]. From eqn. (3), coupled effect between an elastic field and an electric potential field is given in $[\boldsymbol{K}_{u\phi}]$.

2.2 Modelling for Numerical analyses

The effect of interlaminar delamination in composite laminate on electric distribution induced on piezoelectric film was numerically investigated. We consider a CFRP quasi-isotropic laminate plate with an interlaminar delamination throughout the width of the plate and with PVDF film glued on the surface as shown in Figure 1. The laminate is 160 mm in length, 60 mm in width and 7.6 mm in thickness. The laminate has $[(-45/0/45/90)_5]_{\mathrm{s}}$ laminate configuration with 40 unidirectional laminae with thickness of 0.19 mm, here the number in the parentheses indicates the azimuthal angle of the fiber orientation with respect to the X axis; the subscript s denotes that the lamine are symmetrically stacked about the neutral plane. A PVDF layer was located on the 1st layer of the laminate. For simplicity, we assume that the leading edges of delamination are straight and are perpendicular to the length direction of the laminate. Under these assumptions, delamination can be represented by three delamination parameters, i.e. half length of delamination a, lengthwise location of left delamination tip X_{c} and the depth of delamination d. The depth of delamination d is defined as follows. When a delamination exists between the i-th layer and the $(i+1)$-th layer, the depth of delamination is expressed as $d = [i \mid i+1]$. The laminate was subjected to three-point bending. Left and right edges of upper surface are sliding supported and the center point on left supported line is pin supported to prevent rigid body displacement. As an electric

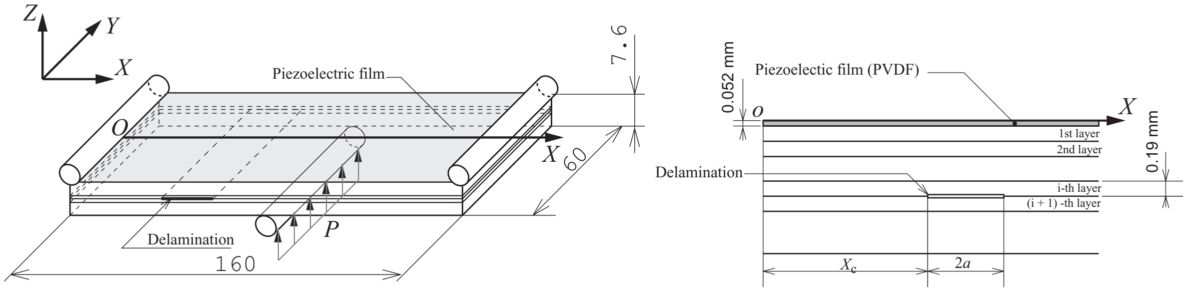

(a) Overall figure (b) Z-X cross-section

Figure 1: Composite laminate for numerical analyses.

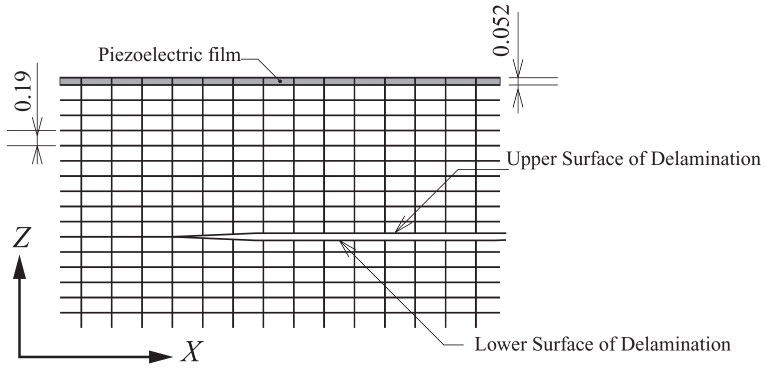

Figure 2: FEM mesh near delamination area (Z-X cross-section).

boundary condition, the potential on the interface between the laminate and the PVDF film is kept to be zero. Distributed load of 1.50×10^4 N/m was applied on mid-length line of lower surface.

The distributions of electric potential induced on the surface of PVDF film were calculated using the foregoing FEM analyses on a personal computer. Figure 2 illustrates Z-X cross-section of the mesh near the delamination area. The laminate was divided into 40 layers along thickness direction so that each layer can represent individual unidirectional laminae. It should be noted that there is no gap between two delaminated surface in the model. Material properties of lamina and PVDF film used in the FEM analysis, which are shown in Tables 1 and 2, are in accordance with the following experiments. In this analysis, lengthwise location of delamination X_{c} and size of delamination a were fixed at 45 mm and 10 mm, respectively, and the electric potential distiribution was calculated for 3 cases of the depth of delamination: $d = [10 \mid 11]$, $[20 \mid 21]$ and $[30 \mid 31]$. An analysis for laminate without defect was also conducted for comparison.

2.3 Calculated Potential Distributions and Discussion

Calculated distributions of electric potential $\phi^{(\mathrm{c})}$ are shown in Figure 3. Superscript (c) indicates that the value is a calculated one. Compared with electric potential distribution for the case without delamination, a characteristic change is observed in the electric potential destribution for the cases with delamination. Figure 4 shows the difference in the electric potential distribution between the case with and without delamination. The difference in electric potential $\Delta\phi$ is defined by

$$\Delta\phi(X) = \phi(X) - \phi_{\mathrm{o}}(X) \tag{5}$$

where ϕ_{o} stands for the electric potential for the laminate without delamination. For all three cases shown in Figure 4, the difference of electric potential $\Delta\phi^{(\mathrm{c})}$ has positive or negative peaks near each

Table 1: Material properties of lamina.

E_1 (GPa)	E_2 (GPa)	E_3 (GPa)	ν_{12}	ν_{23}	ν_{31}	G_{12} (GPa)	G_{23} (GPa)	G_{31} (GPa)
138	9.1	9.1	0.32	0.32	0.02	4.8	3.4	4.8

Table 2: Material properties of PVDF.

(a) Elastic properties ($\times 10^9$ N/m^2)

C_{11}	C_{12}	C_{13}	C_{22}	C_{33}	C_{44}	C_{55}	C_{66}
3.61	1.61	1.42	3.13	1.60	5.50	0.590	0.690

(b) Piezoelectric coefficient properties ($\times 10^{-3}$ C/m^2)

e_{31}	e_{32}	e_{33}	e_{24}	e_{15}
41.0	3.19	−16.2	−12.7	−15.9

(c) dielectric properties ($\times 10^{-10}$ C/Vm)

g_{11}	g_{22}	g_{33}
0.01063	1.063	1.063

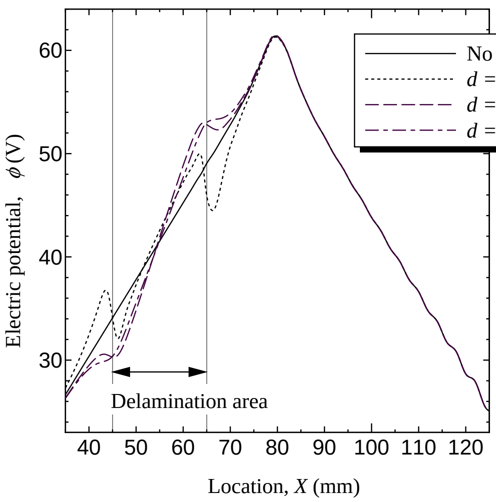

Figure 3: Calculated distribution of electric potential, $\phi^{(c)}$.

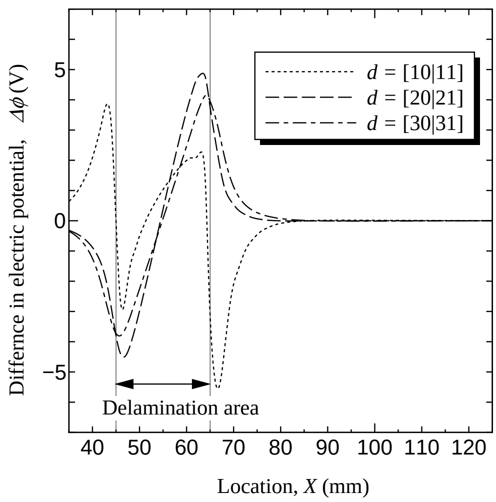

Figure 4: Difference in distribution of calculated electric potential, $\Delta\phi^{(c)}$.

delamination tip. This fact suggests that the location of a delamination tip can be roughly estimated from the peaks of $\Delta\phi$.

Figure 4 also indicates that the depth of delamination d has influence on the electric potential distribution. The $\Delta\phi^{(c)}$ for the case of $d = [10\,|\,11]$ has characteristic distribution compared to other two cases; $\Delta\phi^{(c)}$ for the case of $d = [10\,|\,11]$ has both a positive peak and a negative peak near each delamination tip, while $\Delta\phi^{(c)}$ for the other two cases has a negative peak and a positive peak at the left delamination tip and right delamination tip, respectively. The absolute peak values of $\Delta\phi^{(c)}$ distributions for the case of $d = [20\,|\,21]$ are larger than those for the case of $d = [30\,|\,31]$. These observations suggest that the depth of a delamination d can be estimated from the electric potential distribution on the PVDF film.

3. MEASUREMENT OF ELECTRIC POTENTIAL DISTRIBUTION

3.1 Experimental Procedure

The effect of interlaminar delamination in composite laminate on electric distribution induced on piezoelectric film was experimentally investigated. CFRP $[(-45/0/45/90)_s]_5$ quasi-isotropic laminate specimens made from unidirectional prepregs (TORAY P3312-G) with an artificial delamination were tested. The laminates were 250 mm in length, 60 mm in width and 7.6 mm in thickness. An artificial delamination with the same shape and size as those in the foregoing numerical analysis was artificially introduced using NITOFRON® film of 50 μm thickness during manufacturing. The properties of lamina and PVDF film are the same as those summarised in Tables 1 and 2. The experiment was carried out on the three

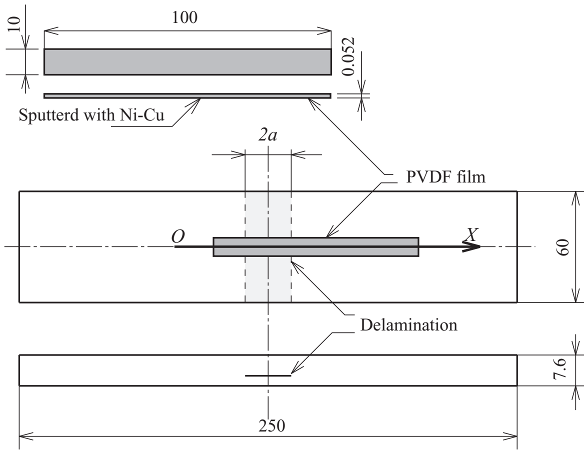

Figure 5: Configuration of specimen.

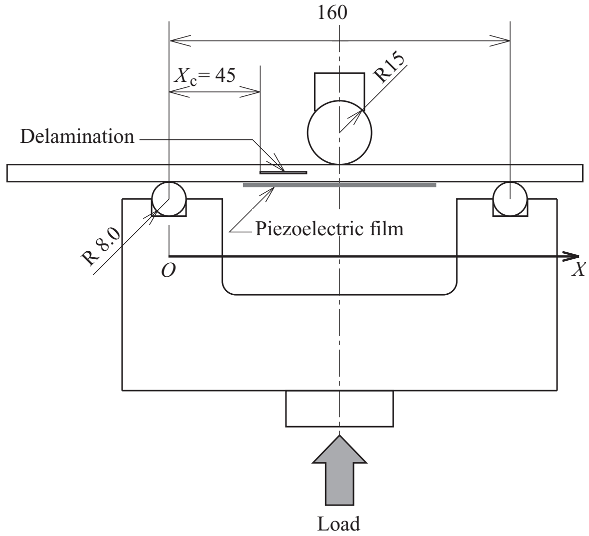

Figure 6: Experimental set-up.

types of specimens which had different depths of delamination: $d = [10 \mid 11]$, $[20 \mid 21]$ and $[30 \mid 31]$. A PVDF film with length of 100 mm, width of 10mm and thickness of 52 μm was glued on the surface of specimens using strain gage adhesive as shown in Figure 5. Adhesive side of the PVDF film was sputtered with Ni-Cu so as to keep the electric potential uniform across the interface between the laminate and the PVDF film.

As is shown in Figure 6, the specimens were placed on a three-point bending apparatus with a span 160 mm and loaded using a servo-hydraulic testing machine at an average load of 980 N, load amplitude of 490 N and load frequency of 3 Hz. It is noted that the specimens were positioned so that lengthwise location of the delamination X_c was 45 mm as shown in Figure 6. Potential distributions induced on surface of the PVDF film were measured using a non-contact voltmeter along the line of mid-width of specimen at the range from $X = 35$ to 125 mm at 0.5 mm interval.

3.2 Measured Electric Potential Distributions and Discussion

Measured distributions of electric potential $\phi^{(\mathrm{m})}$ are shown in Figure 7. Superscript (m) indicates that the value is an experimental one. It is seen in Figure 7 that the measured electric potential distribution shows behavior similar to the calculated electric potential near the delamination tips.

Figure 8 shows the difference in the electric potential distribution between the case with delamination and the case without delamination. The difference in electric potential $\Delta\phi$ was defined by Equation (5). Though electric potential distribution for a specimen without delamination $\Delta\phi_\mathrm{o}$ was not measured in this experiment, it is estimated as follows. In the area of $X \geq 80\,\mathrm{mm}$, the electric potential distribution is not expected to be strongly influenced by the delamination. For a specimen with no delamination, the electric potential distribution is symmetric with respect to the loading line, i.e. $X = 80$. Thus, the electric potential distribution in the area of $X \geq 80\,\mathrm{mm}$ and its mirror image with respect to $X = 80\,\mathrm{mm}$ can be taken as the electric potential distribution for the specimen without delamination. In this study, the electric potential in the area of $X \geq 80$ was fitted by a fourth-order polynomial for smoothing during the process for the estimation of $\phi_\mathrm{o}^{(\mathrm{m})}$. The solid line in Figure 9 illustrates an example of the estimated distribution without a delamination.

For all three cases shown in Figure 7, the difference of electric potential $\Delta\phi^{(\mathrm{m})}$ has positive or negative peaks near each delamination tip. Figure 8 also indicates the effect of the depth of delamination d on the electric potential distribution. As is observed in the foregoing FEM analyses, the $\Delta\phi^{(\mathrm{m})}$ distribution for the case of $d = [10 \mid 11]$ is characteristic compared to the other two cases: $\Delta\phi^{(\mathrm{m})}$ for the case of $d = [10 \mid 11]$ has both a positive peak and a negative peak at the each delamination tip, while $\Delta\phi^{(\mathrm{m})}$ for the other two cases has a negative peak and a positive peak at the left delamination tip and right delamination tip, respectively. However the difference between the $\Delta\phi^{(\mathrm{m})}$ distributions for the case of $d = [20 \mid 21]$ and $[30 \mid 31]$ is smaller than that for the case of $d = [10 \mid 11]$. These observations suggest that if delamination is far from surface where the piezoelectric film is attached, estimation of the depth d becomes difficult.

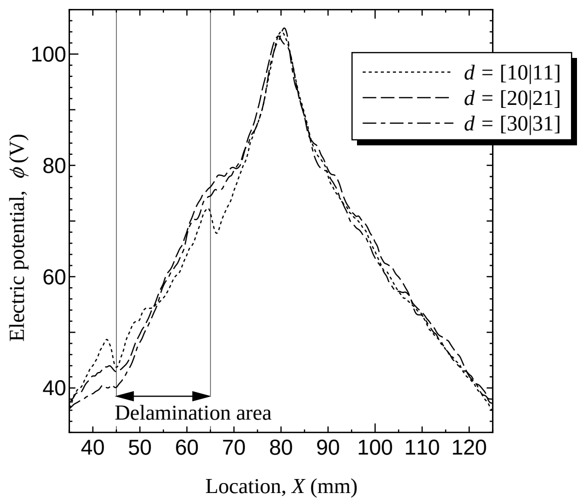

Figure 7: Measured distribution of electric potential, $\phi^{(\mathrm{m})}$.

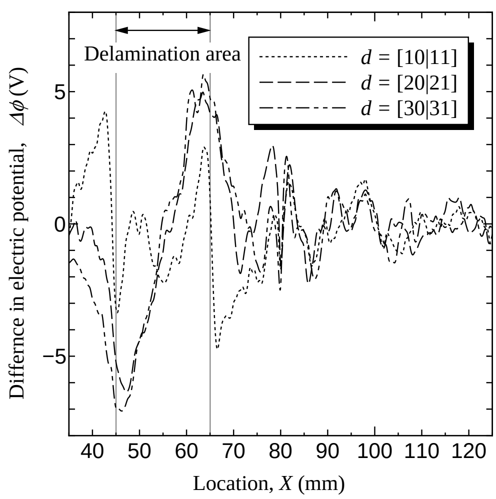

Figure 8: Difference in distribution of measured electric potential, $\Delta\phi^{(\mathrm{m})}$.

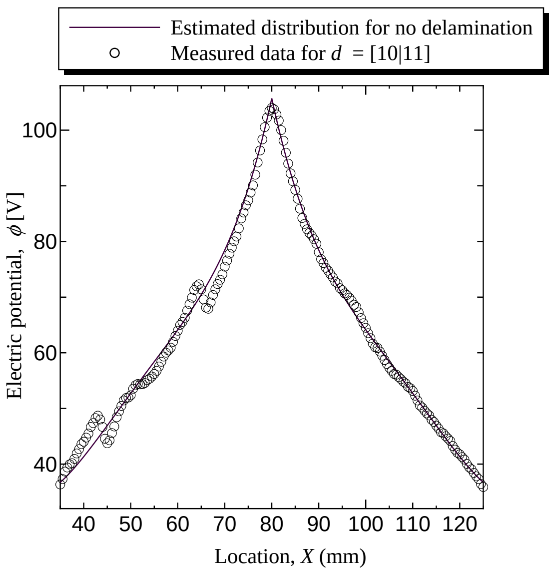

Figure 9: Estimation of electric potential for the specimen without delamination, $\phi_{\mathrm{o}}^{(\mathrm{m})}$.

3.3 Comparison between Experimental and Calculated Electric Potential Distributions

In order to compare the measured electric potential distributions with those obtained by FEM analyses, the electric potential distributions were normalized by the electric potential values on the loading line. Normalized electric potential Φ is defined by,

$$\Phi(X) = \frac{\phi(X)}{\phi_{\mathrm{c}}} \tag{6}$$

where ϕ_{c} is the electric potential value on the surface of piezoelectric film on the loading line of $X = 80\,\mathrm{mm}$. The difference in normalized electric potential between the cases with and without delamination was calculated. Difference in normalized electric potential is given by,

$$\Delta\Phi(X) = \Phi(X) - \Phi_{\mathrm{o}}(X) \tag{7}$$

where Φ_{o} is normalized electric potential for the laminate without delamination.

Distributions of difference in normalized electric potential $\Delta\Phi$ are shown in Figure 10. The agreement between the measured $\Delta\Phi$ distributions and those calculated by FEM analyses is good. However some

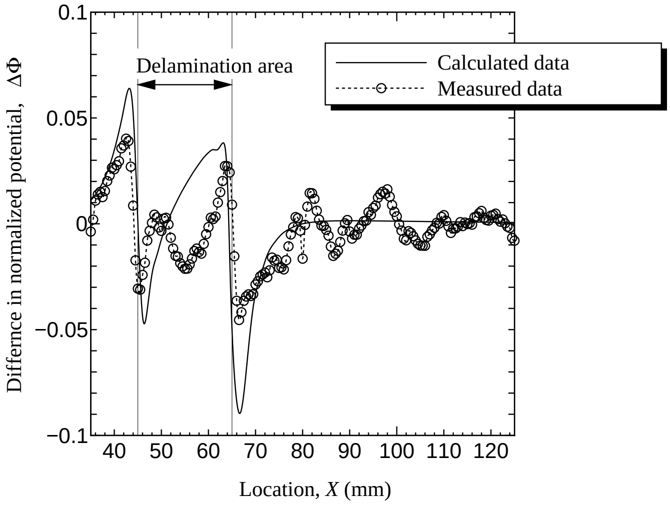

(a) $d = [10|11]$

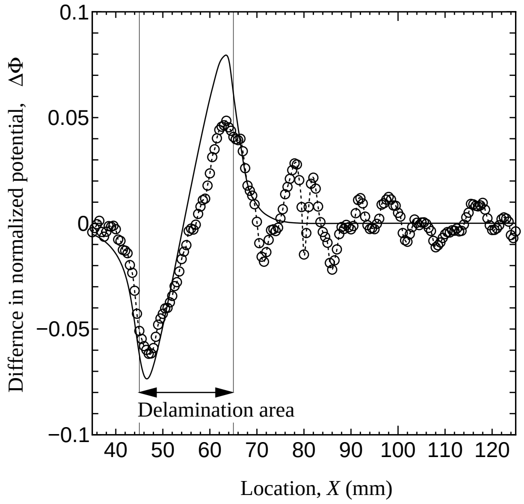

(b) $d = [20|21]$

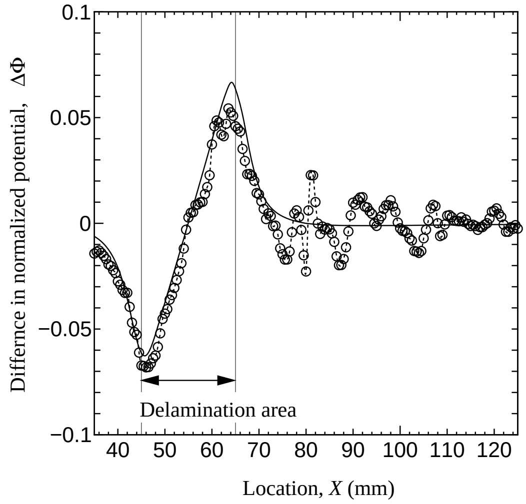

(c) $d = [30|31]$

Figure 10: Difference in normalized potential, $\Delta\Phi$.

absolute values of the peaks in the experimental $\Delta\Phi$ distributions are rather smaller than those in the $\Delta\Phi$ distribution calculated by the FEM. The disagreement is probably attributed to the modeling in FEM. There may be the influence of the fluoropolymer film inserted to introduce the artificial delamination; there may be interference between the upper surface and the lower surface of the fluoropolymer film, while in the FEM model, the upper and the lower surfaces of delamination do not interfere with each other. In addition there is a possibility that the thickness of the fluoropolymer film is not negligible, especially at the delamination tips.

4. IDENTIFICATION OF DELAMINATION

4.1 Method of Delamination Identification

As the inverse analysis method for identification of delaminations, the least squares residual method [6] was applied. In this method, the computed $\Delta\Phi$ distribution and the measured $\Delta\phi$ distribution are compared to determine the most plausible delamination parameter, i.e. the delamination size a, the lengthwise location X_c and the depth of delamination d. As a criterion for identification the following

Table 3: Estimated parameters of delaminations.

(a) Delamination 1

Delamination parameters	a(mm)	X_c(mm)	$X_c + a$(mm)	d	Residual (R_s)
Actual	10.0	45.0	55.0	[10 | 11]	
Estimated	11.2	43.3	44.5	[8 | 9]	
Error	+12%	−1.7 mm	+0.5 (mm)	2/40 layer	2.78×10^{-2}

(b) Delamination 2

Delamination parameters	a(mm)	X_c(mm)	$X_c + a$(mm)	d	Residual (R_s)
Actual	10.0	45.0	55.0	[20 | 21]	
Estimated	8.7	47.3	56.0	[30 | 31]	
Error	−13 %	+2.3 mm	+1.0 (mm)	10/40 layer	1.47×10^{-2}

(c) Delamination 3

Delamination parameters	a(mm)	X_c(mm)	$X_c + a$(mm)	d	Residual (R_s)
Actual	10.0	45.0	55.0	[30 | 31]	
Estimated	9.1	46.6	55.7	[25 | 26]	
Error	−9 %	+1.6 mm	+0.7 (mm)	5/40layer	1.43×10^{-2}

square sum R_s of residual is calculated.

$$R_s(a, X_c, d) = \sum_i^N (\Delta\Phi_i^{(c)}(a, X_c, d) - \Delta\Phi_i^{(m)})^2 \tag{8}$$

Here $\Delta\Phi_i^{(m)}$ denotes the difference in normalized electric potential value measured at the i-th measuring point, and $\Delta\Phi_i^{(c)}(a, X_c, d)$ denotes the difference in normalized electric potential value at the i-th measuring point computed by the FEM, in which delamination parameters are assumed to be a, X_c and d. N is the total number of measuring points. The combination of delamination parameters, which minimize R_s, is employed as the most plausible one among all the assumed combinations of crack parameters.

For effective inverse analysis, the following calculation steps were introduced.

The first step : Delamination parameters are roughly estimated. First, the depth of delamination d is assumed to be d = [10|11], [20|21] or [30|31]. For each depth, R_s is calculated for combinations of 10 delamination lengths a and 6 lengthwise locations X_c ranging from 4 to 13mm and 41 to 51 mm, respectively. It is assumed that R_s is approximated by the following quadratic function of a and X_c.

$$R_s(a, X_c, d) = A + BX_c + Ca + DX_c a + EX_c^2 + Fa^2 \tag{9}$$

Coefficients A, B, C, D, E and F are determined by the least-squares method from the values of R_s for the combinations of 10 delamination lengths and 6 lengthwise locations. For each assumed depth d, the combination of a and X_c, which minimizes R_c is determined based on the approximate function for R_c. Among these combinations of delamination parameters, the combination minimizing R_c is employed as the plausible combination in the rough estimation of delamination parameters.

The second step : The combination of delamination parameters, which gives the minimum of R_s, is searched by using the modified Powell optimization method [13]. The delamination parameters obtained in the above rough estimation are used as the initial values of the crack parameters for the modified Powell method.

4.2. Result of Identification and Discussion

The delamination in CFRP laimnate specimens were identified from the measured electric potential distributions following the foregoing procedure. Actual delamination parameters of specimens tested in the experiment are as follows.

delamination 1 : $(a, X_c, d) = (10, 45, [10|11])$
delamination 2 : $(a, X_c, d) = (10, 45, [20|21])$
delamination 3 : $(a, X_c, d) = (10, 45, [30|31])$

The estimated delamination parameters are shown in Table 3. The errors in the estimated values of a are approximately 10% of the actual delamination length. As for estimation of lengthwise location X_c, it should be noted that X_c is defined as the location of the left delamination edge. If the lengthwise location was defined as the center of the delamination $X_c + a$, there are no substantial errors in the estimation.

The estimated depth of delamination 1 is quite accurate considering the disagreement in absolute values of the peaks between the experimental and the numerical $\Delta\Phi$ distributions. Meanwhile, the error in the estimated depth of delamination 3 is larger than that of delamination 1 though measured $\Delta\Phi$ distribution agrees well with computed distribution for delamination 3. This fact indicates that the accurate estimation of the depth of delamination is difficult, when the delamination is located between layers far from the surface with a piezoelectric film.

5. CONCLUSIONS

The applicability of the passive electric potential CT method to identification of delamination in composite materials was investigated. The effect of interlaminar delamination in composite laminates on electric potential distribution induced on piezoelectric film was investigated both numerically and experimentally. The difference in normalized electric potential $\Delta\Phi$ was defined to compare the electric potential distribution computed by the FEM and measured by the experiment. The computed and measured distribution of $\Delta\Phi$ were in good agreement. In order to identify the delamination from measured electric potential distribution, the inverse method was constructed based on the least squares residual evaluated between the calculated and measured $\Delta\Phi$ distributions. The lengthwise location and size of the delamination were estimated accurately. When the delamination is located between layers close to the surface with piezoelectric film, the accuracy in estimation of the depth of delamination was good. For the estimation of the depth of delamination, the accuracy was deteriorated with increase in the depth. It was shown that the passive electric potential CT method using piezoelectric film was useful for the quantitative identification of interlaminar delamination in laminate composite materials.

Acknowledgement
This work was partly supported by the Ministry of Education, Science, Sports and Culture, Japan under the Grant-in-Aid for Scientific Research.

REFERENCES

1. S.H.D. Valdes and C.Soutis, Delamination detection in composite laminates from variations of their modal characteristics. *J. Sound Vib.* (1999) **1**, 1-9.

2. N. Hu, H. Fukunaga, M. Kameyama, Y. Aramaki, F.K. Chang, Vibration analysis of delaminated composite beams and plates using a higher-order finte element. *Int. J. Mech. Sci.* (2002) **44**, 1479-1503.

3. IEEE Standard on piezoelectricity, 1987, ANSI/IEEE, Std. 176.

4. C.H. Keilers and F.K. Chang, Identifying delaminations in composite beams using built-in piezoelectrics: Part 1 Experiments and analysis. *J. Intelligent Materials and Structures* (1995) **6**, 649-663.

5. C.H. Keilers and F.K. Chang, Identifying delaminations in composite beams using built-in piezoelectrics: Part 2 An identification method. *J. Intelligent Materials and Structures* (1995) **6**, 664-672.

6. S. Kubo, T. Sakagami and K. Ohji, Electric potential CT method based on BEM inverse analyses for measurement of three-dimensional cracks. *Computational Mechanics '86, Proc.of Int.Conf. on Computational Mechanics* (1986) vol.**1**,V-339-V-344.

7. M. Lin and F.K. Chang, The manufacture of composite structures with a built-in network of piezoceramics. *Composite Science Technology* (2002) **62**, 919-939.

8. D.A. Saravanos and D.A. Hopkins, Effects of delaminations on the damped dynamic characteristics of composite laminates: Analysis and experiments. *J. Sound Vib.*, (1996) **5**, 977-993.

9. L. Shanqing, S. Kubo, T. Sakatami and L. Zhengxing, Theoretical and numerical investigations on crack identification using piezoelectric material-embedded structures. *Materials Science Research International* (2000) **6**, 41-48.

10. D. Shiozawa, S. Kubo, T. Sakagami and K. Okuno, An experimental study on applicability of passive electric potential CT method to crack identification. *J. Soc. Material Science Japan* (2000) **8**, 926-931.

11. D. Shiozawa, S.Kubo and T.Sakagami, Passive electric potential CT method using piezoelectric material for crack identification, *Inverse Problems in Science and Engineering.* (2004) **12**, 71-79.

12. D.Shiozawa, S.Kubo and T. Sakagami, An experimental study on applicability of passive electric potential CT method to crack identification, *Proc. of ATEM'03*, September 2003, paper#OS09W0285.

13. W.I. Zangwill, Minimizing a function without calculating derivations. *Computer J.* (1964) **7**, 149-154.